Supplementary Materials of

Polymer-like Inorganic Double Helical Van Der Waals Semiconductor

Jiangbin Wu[1†*], Nan Wang[2†], Ya-Ru Xie[3], Hefei Liu[1], Xinghao Huang[4], Xin Cong[3], Hung-Yu Chen[1], Jiahui Ma[1], Fanxin Liu[5], Hangbo Zhao[4], Jun Zhang[3], Ping-Heng Tan[3], Han Wang[1,2*]

1. Ming Hsieh Department of Electrical and Computer Engineering, University of Southern California, Los Angeles, CA 90089, USA

2. Mork Family Department of Chemical Engineering and Materials Science, University of Southern California, Los Angeles, CA 90089, USA

3.State Key Laboratory of Superlattices and Microstructures, Institute of Semiconductors, Chinese Academy of Sciences, Beijing 100083, China

4. Department of Aerospace and Mechanical Engineering, University of Southern California, Los Angeles, CA 90089, USA

5. Collaborative Innovation Center for Information Technology in Biological and Medical Physics, and College of Science, Zhejiang University of Technology, Hangzhou 310023, P. R. China

† These authors contributed equally to this work.

* jiangbiw@usc.edu (J. W.), han.wang.4@usc.edu (H.W.)

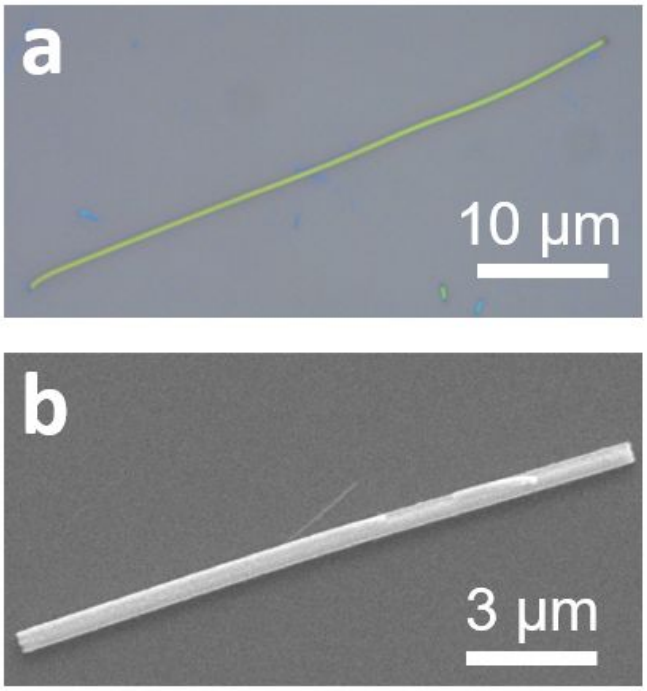

Figure S1. Typical optical microscopy image (a) and scanning electron microscopy image (b) of exfoliated SnIP crystals on the SiO_2/Si substrate.

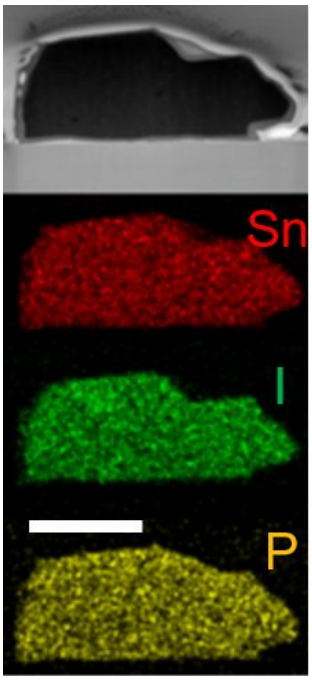

Figure S2. Energy-dispersive X-ray spectroscopy mapping of the cross-section perpendicular to the *a*-axis of the SnIP crystal showing the uniform presence of tin (red), iodine (green), and phosphorus (yellow) elements. The scale bar is 200 nm.

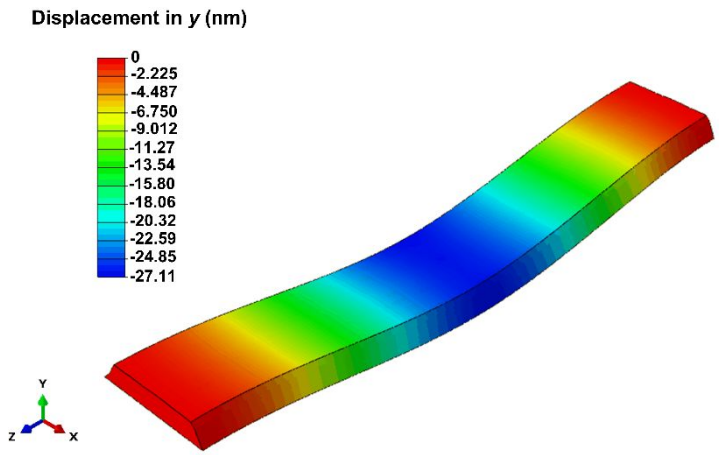

Figure S3. Vertical displacement distribution of a representative SnIP nanowire under an indentation force F=187 nN applied at the center of the nanowire calculated by FEA (deformation scaled by 10x for visualization).

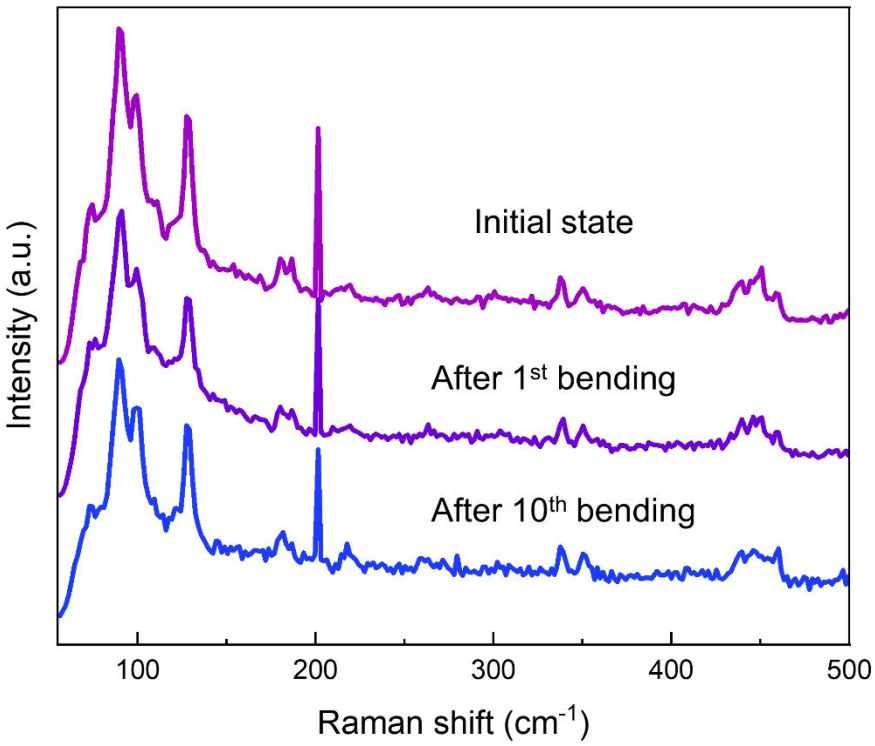

Figure S4. The Raman spectra of SnIP before bending, after 1st bending and after 10th bending test. Both spectra were obtained at the same bent position. It indicates that the materials property remains the same (corresponding to the good repeatability) after 10 times bending.

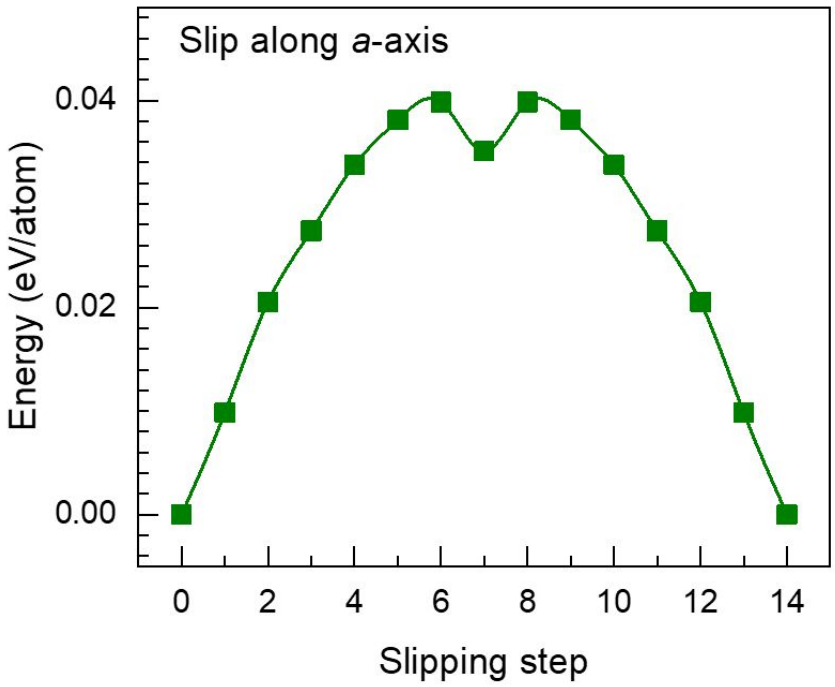

Figure S5. Free energy during the slipping process.

Method

Synthesis of bulk SnIP. Precursor materials, Tin (99.995%, Alfa Aesar), SnI_2 (99.999%, Sigma-Aldrich), and red phosphorus (99.99%, Sigma-Aldrich) were mixed in stoichiometric proportions (Sn:I:P = 1:1:1) with a total weight of 0.4 g and finely ground in an argon-filled environment to form a homogeneous powder, which was then sealed into an evacuated quartz ampoule (~3 mTorr). The ampoule was heated up to 660 °C at a 1.4 °C min^{-1} ramp rate and held at the reaction temperature for 8 hours. The ampule was subsequently cooled down to room temperature with a slow cooling rate of 1 K h^{-1} to obtain crystalline SnIP.

STEM measurement. HR-STEM images were obtained using the FEI Titan Themis G2 system with four detectors and spherical aberration. Chromium and carbon layers were pre-coated on the sample and a thin film was obtained using focused-ion beam (FIB, FEI Helios 450S) with an acceleration voltage of 30 kV. The acceleration voltage was then increased to 200 kV to obtain the HR-STEM image at higher resolutions.

Sample fabrication for the AFM-based nanomechanical bending test. To perform AFM bending tests, SnIP nanowires were acquired by mechanical exfoliation and then transferred on a SiO_2/Si substrate pre-patterned with well-defined circular trenches of varying diameters etched to the depth of 300 nm using reactive-ion etching (RIE). The lengths of the SnIP nanowires are usually around tens micrometers, which is much larger than the diameters of the circular trenches (4 μm). Therefore, the surface of SiO_2/Si substrate that were not etched can provide adequate support to make SnIP nanowires suspend well across the circular trenches after the transfer process. In addition, the metal (Cr/Au) pads with thickness (400 nm) larger than the heights of SnIP nanowires (<300 nm) were deposited at the trench edges to anchor both ends of SnIP nanowires. The bending test on the anchored nanowires was performed using AFM. The effective suspended length is determined from the distance-deformation curve.

Finite element analysis. Simulations for the bending of SnIP nanowire crystals during the AFM measurements were performed using the commercial software ABAQUS. SnIP nanowire geometries with measured cross-sectional profiles were imported. Ten-node tetrahedral (C3D10) elements were adopted with refined mesh (>370,000 elements) to ensure accuracy. Loading was applied along the centreline on the top surface of the nanowires. The bending is in the linear elastic

regime modelled using the fitted Young's modulus and a Poisson's ratio of 0.3 (values of 0.2-0.4 were simulated which showed negligible differences).

DFT calculations. Structural relaxation and stress calculations were performed using Vienna ab initio simulation package (VASP) with the exchange correlation potential of generalized gradient approximation (GGA). To have an accurate stress value, each structure was fully relaxed until the force was below the 0.0001 eV $Å^{-1}$ with k-space mesh of 6 × 6 × 3 and cutoff energy of 500 eV.

The dispersion relations of the acoustic phonon modes were calculated using the DFPT combined with the *phonopy* code.

Brillouin scattering spectroscopy. The Brillouin scattering spectra of SnIP were measured in the backscattering geometry by a confocal microscope system, which is composed of a confocal microscope with a 20× objective lens (numerical aperture=0.42) and the (3+3)-pass tandem Fabry Pérot interferometers with high contrast (~10^{15}). A photon counting head (detector, Hamamatsu H10682-110) is also equipped and the wavelength of incident laser is 532 nm. The linear polarization direction of the incident and scattered beam was tuned by the half wave plate.